Supplementary Information

Mechanical behaviour of large strain capacitive sensor with Barium Titanate Ecoflex composite used to detect human motion.

Eshwar Reddy Cholleti [1,*], Jonathan Stringer[1], Piaras Kelly [2], Chris Bowen [3] and Kean Aw [1]

[1] Department of Mechanical Engineering, University of Auckland, 1010 Auckland, New Zealand
[2] Department of Engineering Science, University of Auckland, 1010 Auckland, New Zealand
[3] Department of Mechanical Engineering, University of Bath, BA2 7AY Bath, UK
***** Correspondence: Eshwar Reddy Cholleti, echo896@aucklanduni.ac.nz

Supplementary Table S1 (ST 1): literature review of interdigital capacitive strain sensors.

Ref	Substrate Material	Dieletric constant of sub-strate	Electrode material	Electrode printing method	Strain	Strain rate	Number of cycles tested	Gauge factor (GF)	Hys-teresis	Capacitance at 0 strain	Influence of substrate mechanical properties on capacitance	App-lication
[1]	PDMS	NR	CNT/PDMS (1/12)	3D printing processes were controlled by Cura Ultimaker software	50 (%)	NR	100	1 mm spacing showed the highest sensitivity and the gauge factors decreased from 0.95 to 0.77 when the strain increased from 10% to 50%.	Not reported	Capacitance increased from 4.93 pF to 20.67 pF when the gap between the electrodes decreased from 3 mm to 1 mm at 100 KHz.	Not reported (N.R)	Tactile and electro-chemical sensing

[2]	Ecoflex® 00-50	4.2	Silver/PVA composite	Laser trenching	63(%)	NR	50	NR	NR	56pF	NR	NR
[3]	Polydimethylsilxane (PDMS)	2.75	CNT-PDMS	Polymer molding	0.35 (%)	NR	1	3.44 – 4.88	NR	1.2 pF	NR	Bending curvature, tactile force and proximity distance
[4]	Polyimide	3.4	Ni/Au	Thin-film technology	2 (%)	NR	1	-1.38	NR	48 pF	NR (E modulus of polymide is 2.5 GPa)	NR
[5]	$Ba_{0.5}Sr_{0.5}TiO_3$	200	Palladium chromium	DC sputtering	0.25 (%)	NR	1	3.13	4.3%	25.7 pF	NR	NR
[6]	PDMS	NR	Cond-uctive PDMS	Multi-step molding	125 (%)	0.2 mm/sec	10	NR	NR	76.8pF at 100 HZ	NR	Characterization of antero-lateral ligment (Bio medical)
[7]	PMMA	4.9	Silver nano-particle ink	Aerosol jet printing	10%	0.1 mm/sec	10	0.663	NR	44.73 pF	NR (Young's modulus of PMMA is 3 GPa)	Structural health monitoring systems
[8]	CeramTec glass ceramic	NR	Ceramtec GC tape	Screen printing	0.3%	NR	1	NR	NR	33.5 pF	NR	NR
[9]	PMMA	NR	gold	Spin-coated and sputtering	0.3%	NR	1	NR	NR	16.4pF	NR	Online monitor-ing CFRP parts.

[10]	Polydimethylsilxane (PDMS)	NR	Ag nanowire	Capillary force lithography (CPL)	30%	NR	1000	-1.57	Value NR	NR	NR	Motion of finger
[11]	Glass-reinforced epoxy laminate material (FR-4)	4.4	silver	Printed circuit board technology	NR	NR	1	NR	NR	11.45pF	NR	To evaluate perm-ittivity of substrate material
[12]	PDMS	2.8	Conductive PDMS (7wt% of MWCNT)	Mold casting	50%	NR	1	NR	NR	6.3pF	NR	NR
[13]	Natural rubber	3	Au (gold)	Photo-lithographic	10%	0.0041 mm/s	1000000	-0.92	NR	23.7pF	NR	Tire strain monitoring for Intelligent tires
[14]	TiO_2/polyvinyl butyral	NR	Silver conduct-ive paste	Deposition method	0.05%	NR	20	2	0.7 %	NR	NR	NR
[15]	Etherester amide elastomer polymer (EEA)	NR	Ag	Direct-write thermal spray technology	0.18%	NR	4	6.8	NR	11.3pF	NR	NR
[15]	Poly-ethylene	NR	Ag	Direct-write thermal spray technology	0.1%	NR	4	0.9	NR	12.4 pF	NR	NR
[16] 2015	PDMS	NR	127-μm thick brass sheet	Laser-micromachining and casting	0.025%	NR	3	6–9	0.6%	14.53 pF	NR	Real time structural health monitoring

Supplementary information of materials and methods:

Preparation of Carbon Black/Ecoflex™ 00-30 Composite Ink

In this work, CB powder with 50 nm particle size (Vulcan® XC72R purchased from Fuel Cell Store, TX, USA) was selected as a conductive phase to fabricate stretchable interdigital capacitor (IDC) electrodes. Commercially available silicone-based polymer (Ecoflex™ 00-30) was used as the flexible and stretchable elastomer medium. The conductivity and printability of CB/Ecoflex™ 00-30 ink is dependent upon the concentration of CB in Ecoflex™ 00-30, and also the amount of added thinners, such as silicone oil.

The CB/Ecoflex™ 00-30 ink was prepared by mixing one part of CB with five parts of Ecoflex™ 00-30 by weight, and diluted with silicone oil, Besil DM 1 Plus (Wacker Chemie AG), in order to achieve the extrusion of CB/Ecoflex™ 00-30 ink through the customized Lulzbot® (Loveland, CO, USA) photo polymer extrusion (PPE) printer nozzle. The ink was mixed with a Kurabo planetary centrifuge mixer (Mazerustar KK-50S). The mixing ratio of CB with Ecoflex™ 00-30 affects the viscosity of CB/Ecoflex™ 00-30 ink. With a small ratio of CB to Ecoflex, the ink viscosity is low and easy to print, but has lower conductivity, while increasing the CB improves the conductivity but increases the ink viscosity. Here, in order to achieve repeatable printing of a high-conductivity ink, 3 mL of silicone oil was added as the thinner to 10 mL of CB/Ecoflex™ 00-30 (1:5 wt%) ink.

Preparation of Ecoflex™ 00-30 and BTO–Ecoflex™ 00-30 Composite Substrates

Three types of substrates were prepared: Ecoflex™ 00-30 with 0, and 40 wt% 100 nm and 200 nm BTO. The BTO nano-particles (100 nm and 200 nm) purchased from TPL Inc. (Albuquerque, NM, USA) were initially manually mixed with Ecoflex™ 00-30, and then homogenously dispersed in the Ecoflex™ 00-30 using a planetary mixer (Mazerustar KK-50S). The mixture was then poured into an acrylic mold and left to cure at room temperature for a minimum of 12 h. The loading of BTO was limited to 40 wt% based upon preliminary experiments that demonstrated that when the amount of BTO reached 50% by weight, the composite substrate took an extremely long time to cure and broke easily at the first cycle of the stretch test. A 50 wt% BTO would be approximately 14.5 vol% of the total volume, which approaches the theoretical percolation volume percentage of spheres of 16%. At such high solid loadings of BTO, it is likely that there would be large agglomerated regions of BTO within the substrate, which would result in likely points of failure under mechanical loading. Fatigue testing demonstrated that substrates with 40 wt% BTO or lower in the Ecoflex survived the 1000 stretch and relax (100% strain) cycle. Hence, up to 40 wt% (approximately 6.8 and 10.1 vol%) BTO in Ecoflex were examined.

The conformal mapping technique is the most suitable method to calculate the capacitance of IDC structures. The conformal mapping technique provides closed form expressions for the computation of the capacitance of IDC electrodes based on the geometries of the sensor as shown in Figure 3.

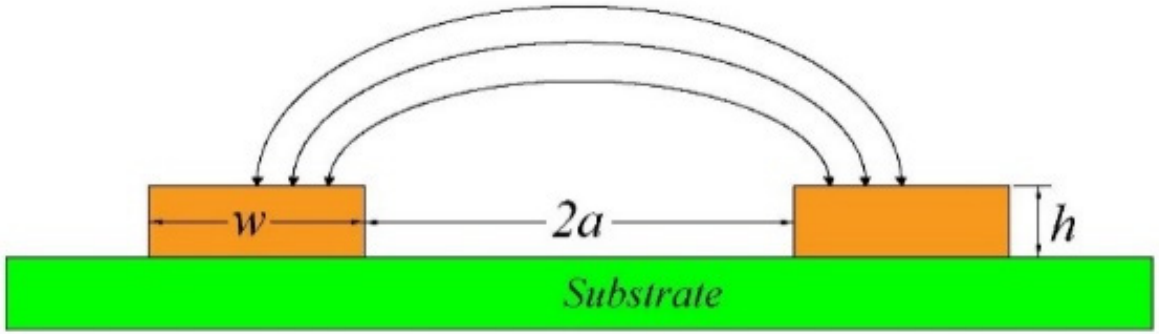

Supplementary Figure S1 (SF 1): Cross-section view of coplanar strip line with fringing electric field.

Supplementary Table S2 (ST 2): Capacitance and relative permittivity of 40 wt % 200 nm BTO.

	200 nm BTO	
	Calculated	**Experimental**
Capacitance - (pF)	26.50	31.4
Relative Permittivity	5.98	7.09

The performance of the sandwiched IDC as a highly stretchable capacitive sensor depends on the electrode overlap length l, width w, height h, and electrode spacing s. The actual printed dimensions of the IDC are summarized in ST3.

Supplementary Table S3 (ST 3) : The actual dimensions of the printed IDC, dimensions in mm.

Dimension (mm)	Overlap Length, l	Width, w	Height, h	Spacing, s
Average	19.50 ± 0.06	0.58 ± 0.13	0.26 ± 0.07	1.06 ± 0.01
Designed dimension	20.00	0.33	0.33	1.50

From ST3, it can be seen that the actual dimensions of the printed IDC deviated slightly from the designed dimensions. The extruded CB/EcoflexTM 00-30 ink flattened slightly due to a combination of gravitational and capillary forces, causing the width to be wider and the height to be lower. This also made the spacing between the electrodes smaller than designed. A typical cross section of the printed electrodes is shown in SF 2.

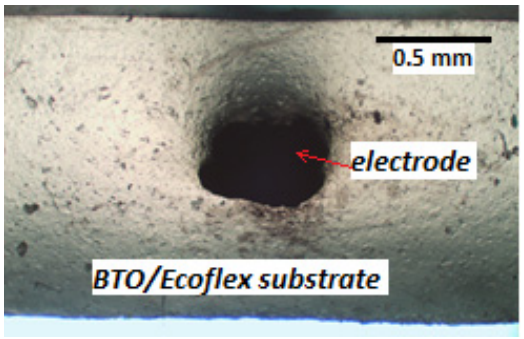

Supplementary Figure S2 (SF 2): A cross section of the printed carbon black (CB)/Ecoflex electrode.

An SEM image of a cross section of 200 nm BTO–EcoflexTM 00-30 composite substrate and printed CB/Ecoflex electrodes is shown in SF 3. It does not show any significant surface roughness in the substrate, indicating that the BTO was reasonably well-distributed within the Ecoflex matrix.

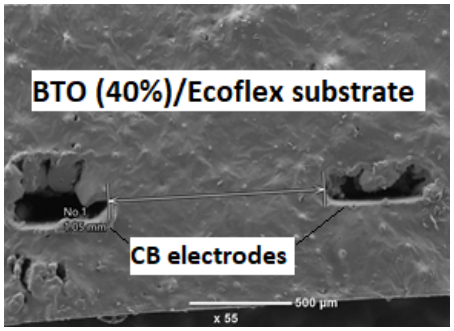

Supplementary Figure S3 (SF 3): SEM image of a cross section of 200 nm BTO–Ecoflex™ 00-30 composite substrate and printed CB/Ecoflex electrode.

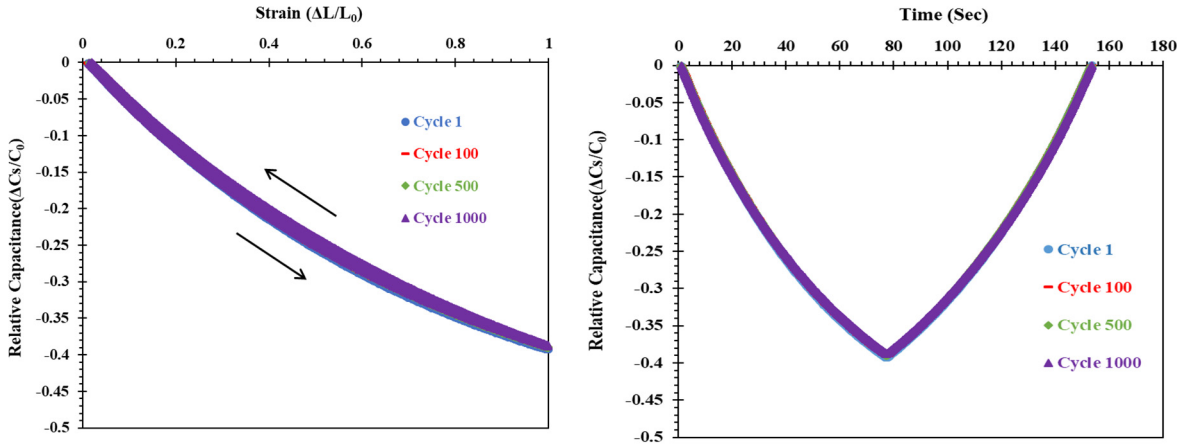

Supplementary Figure S4 (SF 4): IDC sensor with pristine Ecoflex 00-30™ substrate tested at 0.7 mm per sec, (**a**) The relative change in capacitance ($\Delta C_s/C_0$) strained up to 100% after 1, 100, 500 and 1000 stretch/relax cycles. (**b**) The $\Delta C_s/C_0$ versus time as the sensor was stretched to 100% strain.

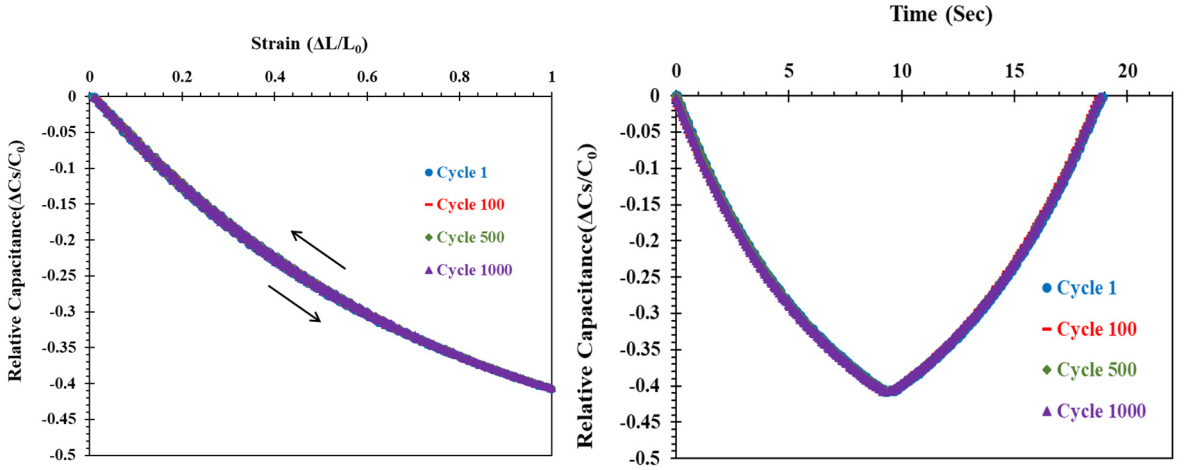

Supplementary Figure S5 (SF 5): IDC sensor with pristine Ecoflex 00-30™ substrate tested at 7 mm per sec, (a) The relative change in capacitance ($\Delta C_s/C_0$) strained up to 100% after 1, 100, 500 and 1000 stretch/relax cycles. (b) The $\Delta C_s/C_0$ versus time as the sensor was stretched to 100% strain.

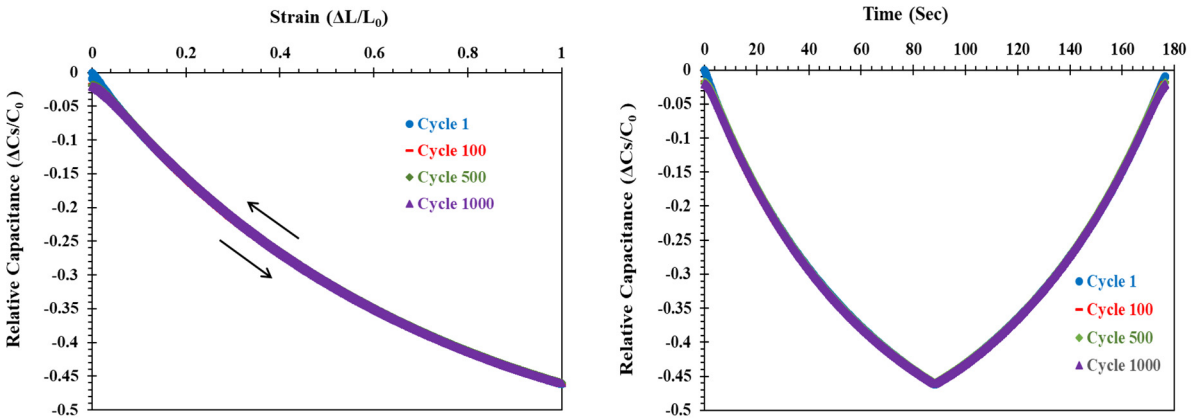

Supplementary Figure S6 (SF 6): IDC sensor with 40 wt % 200 nm BTO-Ecoflex 00-30™ substrate tested at 0.7 mm per sec, (a) The relative change in capacitance ($\Delta C_s/C_0$) strained up to 100% after 1, 100, 500 and 1000 stretch/relax cycles. (b) The $\Delta C_s/C_0$ versus time as the sensor was stretched to 100% strain.

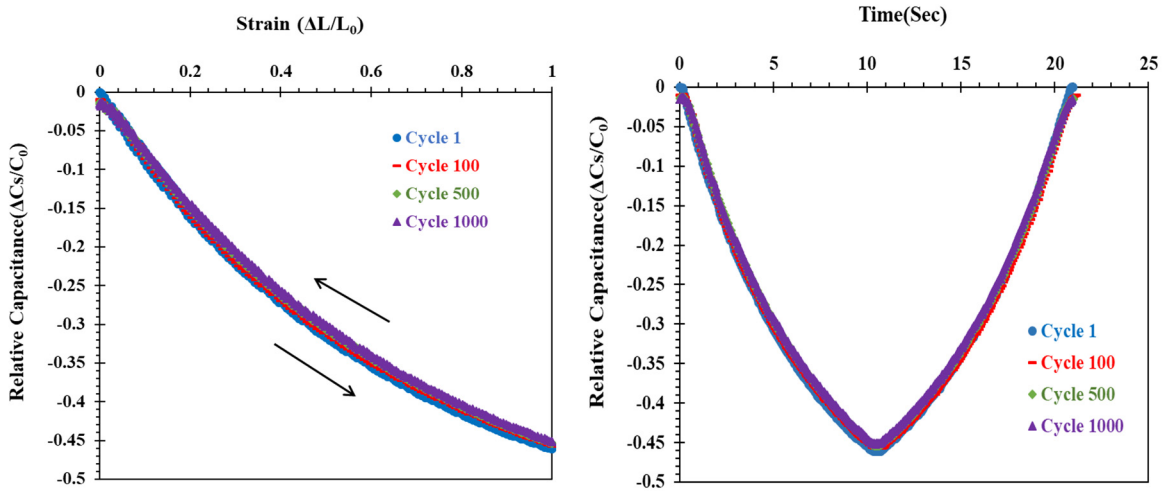

Supplementary Figure S7 (SF 7): IDC sensor with 40 wt % 200 nm BTO-Ecoflex 00-30™ substrate tested at 7 mm per sec, (a) The relative change in capacitance ($\Delta C_s/C_0$) strained up to 100% after 1, 100, 500 and 1000 stretch/relax cycles. (b) The $\Delta C_s/C_0$ versus time as the sensor was stretched to 100% strain.

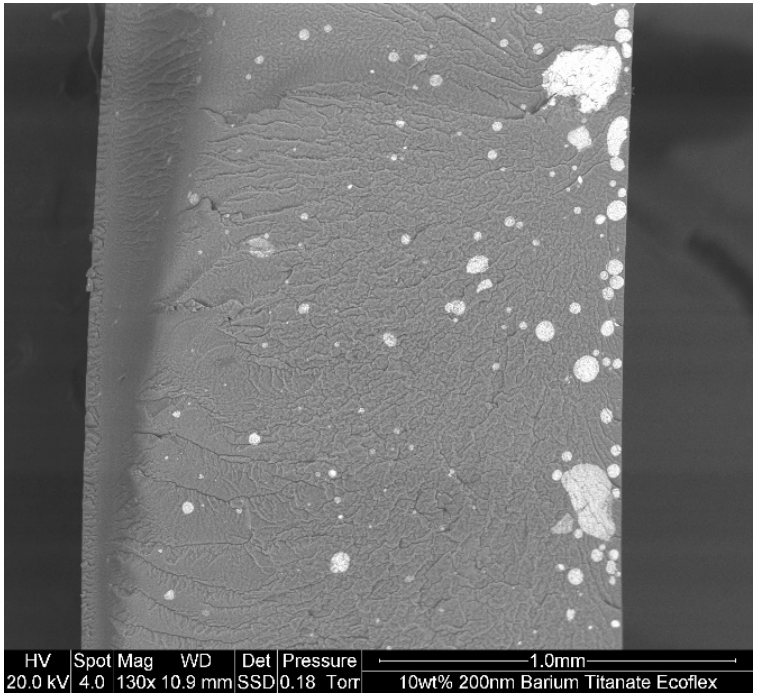
HV
20.0 kV
Spot Mag
4.0 130x
WD
10.9 mm
Det
SSD
Pressure
0.18 Torr
1.0mm
10wt% 200nm Barium Titanate Ecoflex

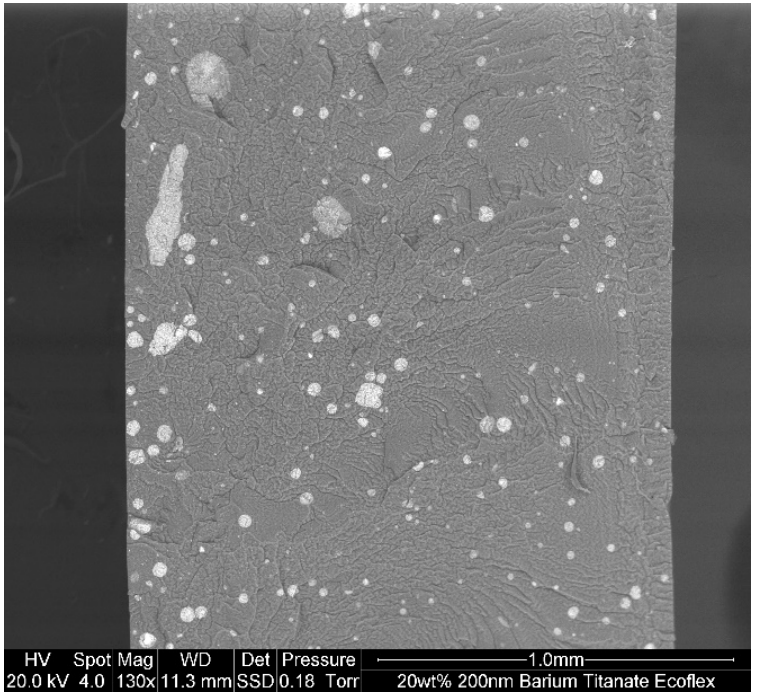
HV
20.0 kV
Spot Mag
4.0 130x
WD
11.3 mm
Det
SSD
Pressure
0.18 Torr
1.0mm
20wt% 200nm Barium Titanate Ecoflex

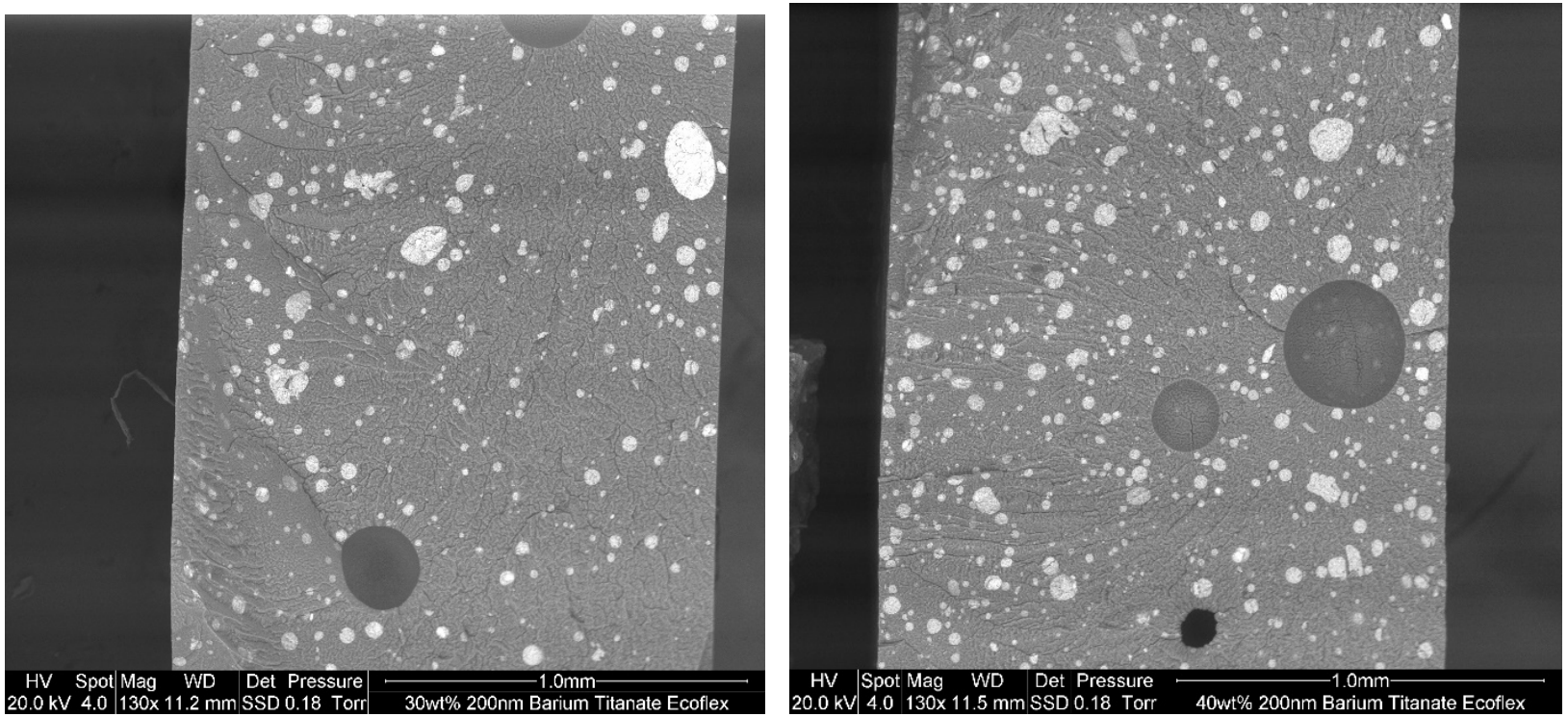

The distribution of the BTO in Ecoflex is gradually increasing with incrasing the loading of BTO from 10 wt % to 40 wt % and at less loading of BTO (10 and 20 wt%) the sedementation of BTO is observed

Supplementary Figure S8 (SF8): Scanning electron microscope (SEM) analysis of 10 wt %, 20 wt %, 30 wt % and 40 wt % of 200 nm BTO-Ecoflex composite with 1mm scale of magnification.

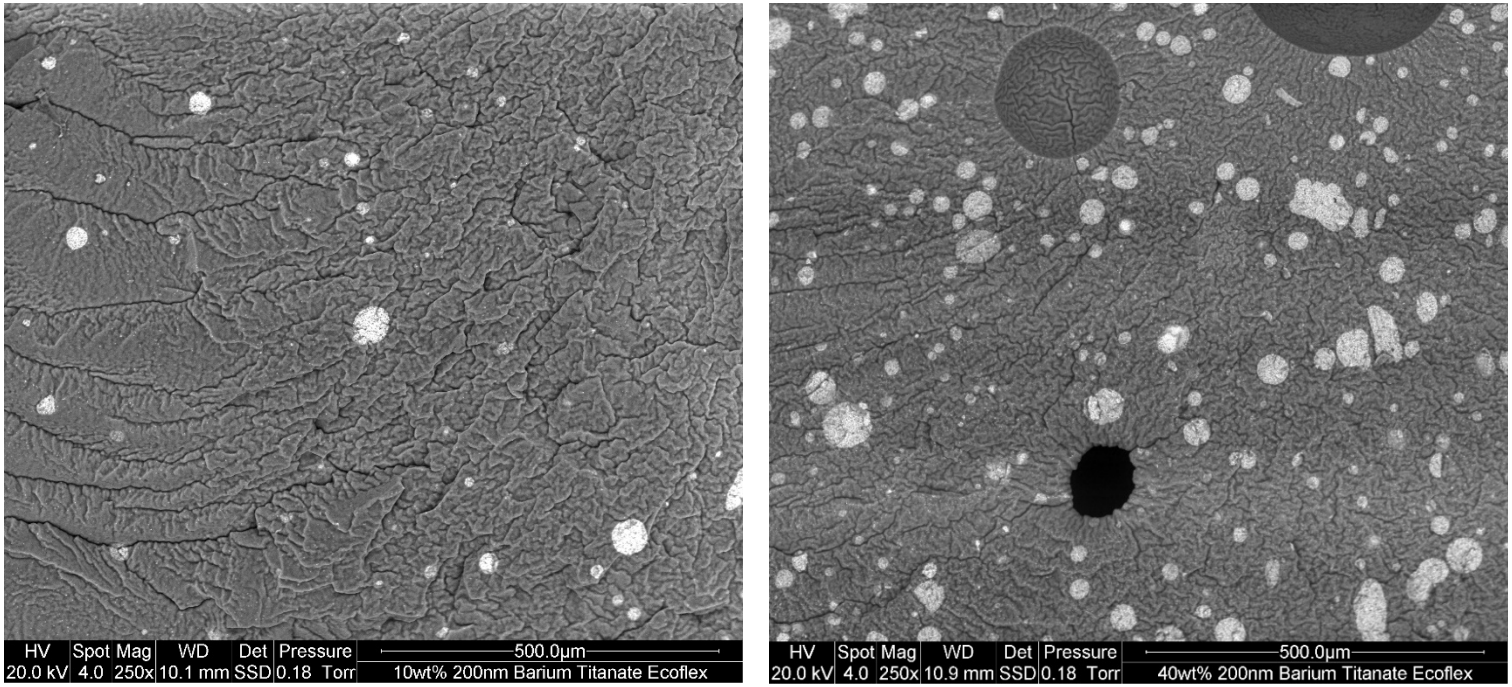

It is evident from the SEM analysis of 10 wt % and 40 wt % of 200 nm BTO-Ecoflex composites that even though there are agglomerations of BTO, the distribution of BTO filler is more uniform than the 10 wt % BTO because the surplus BTO filler at higher loading.

Supplementary Figure S9 (SF9): Scanning electron microscope (SEM) analysis of 10 wt %, and 40 wt % of 200 nm BTO-Ecoflex composite with 500 µm scale of magnification.

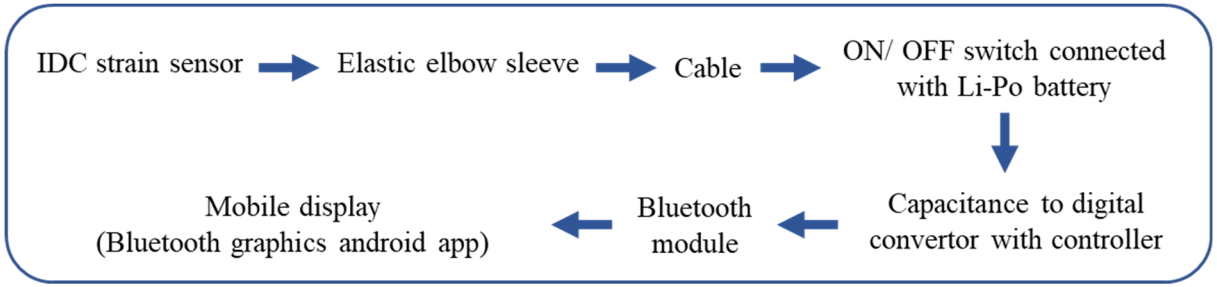

Supplementary Figure S10 (SF 10): Flow chart of developing the application with IDC sensor to measure the elbow angle.

Reference:

[1] K. Li, H. Wei, W. G. Liu, H. Meng, P. X. Zhang, and C. Y. Yan, "3D printed stretchable capacitive sensors for highly sensitive tactile and electrochemical sensing," *Nanotechnology,* vol. 29, no. 18, May 4, 2018.

[2] T. Houghton, J. Vanjaria, T. Murphy, and H. B. Yu, "Stretchable Capacitive Strain Sensors Based on a Novel Polymer Composite Blend," *2017 Ieee 67th Electronic Components and Technology Conference (Ectc 2017)*, pp. 2263-2268, 2017.

[3] C. F. Hu, J. Y. Wang, Y. C. Liu, M. H. Tsai, and W. L. Fang, "Development of 3D carbon nanotube interdigitated finger electrodes on polymer substrate for flexible capacitive sensor application," *Nanotechnology,* vol. 24, no. 44, Nov 8, 2013.

[4] R. Zeiser, T. Fellner, and J. Wilde, "Capacitive strain gauges on flexible polymer substrates for wireless, intelligent systems," *J. Sens. Sens. Syst.,* vol. 3, no. 1, pp. 77-86, 2014.

[5] S. Ren, S. Jiang, H. Liu, W. Zhang, and Y. Li, "Investigation of strain gauges based on interdigitated Ba0.5Sr0.5TiO3 thin film capacitors," *Sensors and Actuators A: Physical,* vol. 236, pp. 159-163, 2015/12/01/, 2015.

[6] M. Zens, J. Ruhhammer, F. Goldschmidtboeing, M. J. Feucht, A. Bernstein, P. Niemeyer, H. O. Mayr, and P. Woias, "Polydimethylsiloxane Strain Gauges for Biomedical Applications," *2015 Transducers - 2015 18th International Conference on Solid-State Sensors, Actuators and Microsystems (Transducers)*, pp. 1763-1766, 2015.

[7] K. T. Fujimoto, J. K. Watkins, T. Phero, D. Litteken, K. Tsai, T. Bingham, K. L. Ranganatha, B. C. Johnson, Z. Deng, B. Jaques, and D. Estrada, "Aerosol jet printed capacitive strain gauge for soft structural materials," *npj Flexible Electronics,* vol. 4, no. 1, pp. 32, 2020/11/23, 2020.

[8] N. Blaz, M. Kisic, C. Zlebic, G. Miskovic, G. Radosavljevic, and L. Zivanov, "Displacement Sensor Based on Interdigital Capacitor," *2015 38th International Spring Seminar on Electronics Technology (Isse 2015)*, pp. 477-481, 2015.

[9] M. Hubner, D. Grabner, A. Ozdemir, and W. Lang, "Influence of strain on miniaturized flexible sensor for on-line monitoring of CFRP production," *4th International Conference on System-Integrated Intelligence: Intelligent, Flexible and Connected Systems in Products and Production,* vol. 24, pp. 173-178, 2018.

[10] S. R. Kim, J. H. Kim, and J. W. Park, "Wearable and Transparent Capacitive Strain Sensor with High Sensitivity Based on Patterned Ag Nanowire Networks," *Acs Applied Materials & Interfaces,* vol. 9, no. 31, pp. 26407-26416, Aug 9, 2017.

[11] Y. Z. Huang, Z. Zhan, and N. Bowler, "Optimization of the Coplanar Interdigital Capacitive Sensor," *43rd Review of Progress in Quantitative Nondestructive Evaluation,* vol. 1806, 2017.

[12] H. S. Shin, and S. Bergbreiter, "Effect of finger geometries on strain response of interdigitated capacitor based soft strain sensors," *Applied Physics Letters,* vol. 112, no. 4, Jan 22, 2018.

[13] R. Matsuzaki, T. Keating, A. Todoroki, and N. Hiraoka, "Rubber-based strain sensor fabricated using photolithography for intelligent tires," *Sensors and Actuators a-Physical,* vol. 148, no. 1, pp. 1-9, Nov 4, 2008.

[14] A. Arshak, K. Arshak, D. Morris, O. Korostynska, and E. Jafer, "Investigation of TiO2 thick film capacitors for use as strain gauge sensors," *Sensors and Actuators a-Physical,* vol. 122, no. 2, pp. 242-249, Aug 26, 2005.

[15] J. Li, J. P. Longtin, S. Tankiewicz, A. Gouldstone, and S. Sampath, "Interdigital capacitive strain gauges fabricated by direct-write thermal spray and ultrafast laser micromachining," *Sensors and Actuators a-Physical,* vol. 133, no. 1, pp. 1-8, Jan 8, 2007.

[16] H. Cao, S. K. Thakar, M. L. Oseng, C. M. Nguyen, C. Jebali, A. B. Kouki, and J. C. Chiao, "Development and Characterization of a Novel Interdigitated Capacitive Strain Sensor for Structural Health Monitoring," *Ieee Sensors Journal,* vol. 15, no. 11, pp. 6542-6548, Nov, 2015.